

Testing statics-dynamics equivalence at the spin-glass transition in three dimensions

Luis Antonio Fernández and Víctor Martín-Mayor

*Departamento de Física Teórica I, Universidad Complutense, 28040 Madrid, Spain**and Instituto de Biocomputación y Física de Sistemas Complejos (BIFI), Zaragoza, Spain*

(Received 19 December 2014; revised manuscript received 11 May 2015; published 26 May 2015)

The statics-dynamics correspondence in spin glasses relate nonequilibrium results on large samples (the experimental realm) with equilibrium quantities computed on small systems (the typical arena for theoretical computations). Here we employ statics-dynamics equivalence to study the Ising spin-glass critical behavior in three dimensions. By means of Monte Carlo simulation, we follow the growth of the coherence length (the size of the glassy domains), on lattices too large to be thermalized. Thanks to the large coherence lengths we reach, we are able to obtain accurate results in excellent agreement with the best available equilibrium computations. To do so, we need to clarify the several physical meanings of the dynamic exponent close to the critical temperature.

DOI: [10.1103/PhysRevB.91.174202](https://doi.org/10.1103/PhysRevB.91.174202)

PACS number(s): 75.10.Nr, 75.40.Gb, 75.40.Mg

The glass transition, the dramatic dynamic slowdown experienced by spin glasses, fragile molecular glasses, polymers, colloids, etc., upon approaching their glass temperature T_g , has long puzzled scientists [1]. The phenomenon has been long suspected to be caused by the growth of a characteristic length [2], an issue under current investigation [3–5].

Spin glasses enjoy a privileged status in this context, for a number of reasons. *First*, their glass transition is a *bona fide* phase transition at $T_c = T_g$ [6–8]. *Second*, consider a rapid quench from high temperature to the working temperature $T < T_c$, where the system is left to equilibrate for a time t_w . The system remains perennially out of equilibrium. This *aging* process [9] consists of the growth of glassy magnetic domains (which reminds us of coarsening [10]). The size of these domains $\xi(t_w)$ is experimentally accessible, and it can be as large as 100 lattice spacings [11,12] (enormously larger than any length scale identified on molecular liquids [4,5]). *Third*, the growth of $\xi(t_w)$ has been well studied numerically [13–22]. In particular, the dedicated Janus computer [23] has allowed us to cover t_w ranging from picoseconds to 0.1 s [20,21]. *Fourth*, a statics-dynamics correspondence is expected [24]: detailed dictionaries have been built [25,26], relating equilibrium results on finite systems (the typical setting for numerical simulations) with nonequilibrium results on macroscopic (or mesoscopic) samples.

The statics-dynamics equivalence is particularly exciting, because it brings the much awaited possibility of detailed comparisons between experimental results and theoretical computations. In fact, experimental effort has been recently devoted to the measurement of $\xi(t_w)$ with that end [11,12,27–29]. Unfortunately, appealing as it is, the statics-dynamics equivalence has not yet produced new insights (in fact, not even the mutual consistency of different dictionaries [25,26] has been shown).

Here we obtain a complete characterization of the critical behavior of the three-dimensional Ising spin glass based solely on the statics-dynamics equivalence. Our Monte Carlo simulations follow the growth of $\xi(t_w)$ on lattices too large to be equilibrated. In this way, we obtain the largest coherence lengths ever obtained in a simulation (up to 25 lattice spacing). Thus armed, we obtain fairly accurate estimates of the critical exponents. Our results are completely consistent with the

best *equilibrium* computations on small lattices [30,31]. Our analysis is obviously related to dynamic scaling [32], with an important difference. We find it mandatory to eliminate time, in favor of the coherence length $\xi(t_w)$. The reason, explained below, is that the dynamic exponent z changes its physical meaning at T_c . Last, but not least, we show in Appendix A how to perform on conventional processors investigations previously regarded as impossible without special computers.

The Hamiltonian for the $D=3$ Edwards-Anderson model with nearest-neighbors interactions is

$$\mathcal{H} = - \sum_{\langle x,y \rangle} J_{x,y} \sigma_x \sigma_y. \quad (1)$$

The spins $\sigma_x = \pm 1$ are placed on the nodes x of a cubic lattice of linear size $L = 256$ and periodic boundary conditions. The couplings $J_{x,y} = \pm 1$ are chosen randomly with 50% probability, and are quenched variables. Each coupling choice is named a *sample*. We denote by $\langle \dots \rangle$ the average over the couplings. Model (1) undergoes a spin-glass transition at $T_c = 1.1019(29)$ [31].

We study the direct quench, the simplest dynamic protocol. At the starting time $t_w = 0$, the system is in a random configuration (i.e., $T = \infty$). We place it instantaneously at the working temperature T and follow the evolution as t_w increases, Fig. 1. Our time unit is the Monte Carlo step (a full lattice Metropolis sweep).¹

Metropolis dynamics belongs to the universality class of the physical evolution (it is an instance of the so-called model A dynamics [33]), and is straightforward to implement [34]. However, our aim is to reach large L and t_w . Rather than resorting to special hardware [22,23,35–37], we employ synchronous multispin coding on standard CPUs. In a naive implementation random number generation is a major cost. However, our minimal energy barrier is 4, rarely overcome

¹We have simulated the same 50 samples at $T = 1.5$ ($t_w \leq 2^{23}$), $T = 1.4$ ($t_w \leq 2^{25}$), $T = 0.5, 0.6, 0.7, 0.8$ ($t_w \leq 2^{26}$), $T = 0.9, 1.2, 1.25, 1.3$ ($t_w \leq 2^{28}$), and at $T = 1.0, 1.1, 1.15$ ($t_w \leq 2^{29}$). For each sample we simulate four independent systems (replicas), $\{\sigma_x^{(a)}\}$ $a = 1, \dots, 4$ [eight replicas at $T = 1.1 \approx T_c$, and (to control the possibility of thermalization effects) at $T = 1.25$].

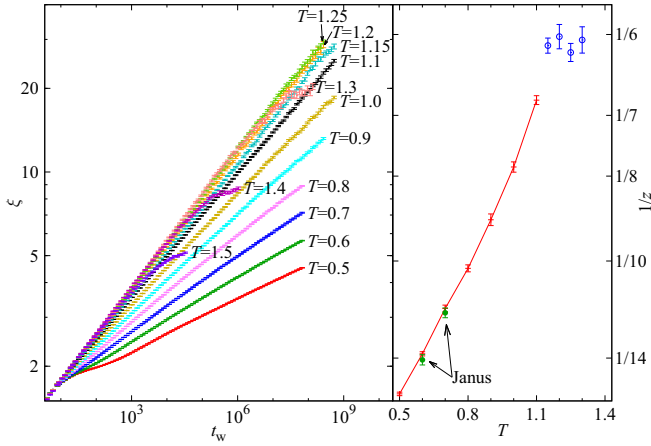


FIG. 1. (Color online) Left: Coherence length $\xi_{12}(t_w)$ vs Monte Carlo time, as computed for model (1) on lattices of size $L = 256$, for several temperatures ($T_c = 1.1019(29)$ [31]). One Monte Carlo step corresponds to 1 ps in physical time [43]. For $T \geq 1.3$, we reach equilibrium. Right: Dynamic exponent $z(T)$ computed in the nonequilibrium regime $\xi(t_w) \sim t_w^{1/z(T)}$. Joined red points stand for $T \leq T_c$. Note the constant value $z(T > T_c) \approx 6$ (blue circles). We perform the fits for $t_w > 2^{20} \approx 10^6$ Monte Carlo steps (but for $T = 1.3$ where $2^{16} \leq t_w \leq 2^{20}$, in order to avoid thermalization). We also show Janus data [21] (green circles) computed for longer times. We only show the $L = 80$ Janus data at temperatures free from finite-size artifacts.

at the temperatures of interest [for instance, $\exp(-4/T_c) \approx 0.026$]. Hence, the Gillespie method [38,39] allows for major savings (see Appendix A).²

We compute the coherence length from the correlation function of the replica field $q_x(t_w) \equiv \sigma_x^{(a)}(t_w)\sigma_x^{(b)}(t_w)$:³

$$C_4(\mathbf{r}, t_w) = L^{-3} \sum_x q_x(t_w) q_{x+\mathbf{r}}(t_w). \quad (2)$$

We restrict the displacement \mathbf{r} to a lattice axis and compute integrals $I_k(t_w) = \int_0^\infty dr r^k C_4(\mathbf{r}, t_w)$. Then $\xi_{1,2}(t_w) = I_2(t_w)/I_1(t_w)$ [20,21]. In all cases, we find $L > 10 \xi_{1,2}(t_w)$ hence we regard our data as representative of the thermodynamic limit [20].

Figure 1 shows a rather accurate algebraic growth $\xi(t_w) \sim t_w^{1/z(T)}$ [11,15].⁴ Yet there is some controversy. On the one hand, low-temperature data suggest $z(T \leq T_c) \approx z_c T_c/T$ [11,15,20,21]. On the other hand, in Ref. [41] a temperature varying protocol with $T \geq T_c$ produced a numerical value [$z_c = 5.85(9)$ for $J = \pm 1$ or $z_c = 6.00(19)$ for Gaus-

sian couplings] hardly consistent with the low-temperature $z_c = 6.86(16)$ [20,21].

Our own data, Fig. 1 right, suggest an exponent $z(T)$ discontinuous at T_c . Of course this might be an effect of our $z(T)$ being an effective exponent (due to our fitting time window). But this is not a logical necessity.

Indeed, exponent $z(T)$ carries different meanings. For $T < T_c$ it describes (glassy) coarsening: the coherence length grows forever as $\xi(t_w) \sim t_w^{1/z(T)}$. Yet $z(T > T_c)$ is concerned with equilibration. One has a characteristic time $\tau(T)$ [when $\xi(\tau, T)$ reaches, say, 90% of the equilibrium ξ_{eq}] and then $\tau(T) \propto [\xi_{eq}(T)]^{z^*}$. In fact, for the simplest nontrivial model (the $D = 2$ Ising ferromagnet) the coarsening exponent is $z_{FM}(T < T_c^{FM}) = 2$ [10], while $z_{c,FM}^* = 2.1667(5)$ [42] for critical equilibration.

Clearly this delicate crossover will require further investigation. Yet we have rationalized why a $T \geq T_c$ protocol [41] produces $z(T > T_c) \approx 6$.

These complications reinforce our choice of basing finite-time scaling on $\xi_{1,2}(t_w)$, rather than on t_w [32,44,45]. To do so, we adapt Binder's method [46] (in Appendix C we explore another possibility [47] that turns out to be less accurate). Let $q(B_l, t_w) = \sum_{x \in B_l} q_x(t_w)/l^3$ be the average of the replica field on a cubic box of side l . We compute $q_k(l, t_w) = \overline{q^k(B_l, t_w)}$, its k th power averaged over samples, replica pairings, as well as over boxes B_l . Binder's ratio $U_4(l, t_w, T) = \overline{q_4(l, t_w)}/\overline{q_2(l, t_w)}^2$ is a dimensionless parameter likely to display universal behavior (for instance, $U_4(l, t_w, T) \rightarrow 3$ when $l \gg \xi(t_w)$ due to the central limit theorem, see also Ref. [48]).

The analogy with finite size scaling impels us to change variables: $y = [T - T_c][\xi(t_w, T)]^{1/\nu}$ and $\lambda = l/\xi(t_w, T)$. Then, barring subleading corrections to scaling, we expect

$$U_4(l, t_w, T) = f(y, \lambda) + [\xi(t_w)]^{-\omega} g(y, \lambda), \quad (3)$$

where ν is the correlation-length critical exponent, ω is the leading corrections to scaling exponent, and f and g are dimensionless scaling functions. Note that the independent variables in the left-hand side of Eq. (3) (l , t_w , and T) are discrete. Yet the right-hand side variables (y , λ) are continuous. We solve this problem by means of polynomial interpolations (see Appendix B). Errors are estimated with the jackknife method [49], computed over the samples.

Figure 2 contains a qualitative discussion of Eq. (3). In the inset we show data at $y = 0$ (i.e., $T = 1.1$, an excellent approximation to T_c [31]). For large $\xi(t_w)$, U_4 converges to the scaling function $f(0, \lambda)$. On the other hand, in Fig. 2 (main) we show that Eq. (3) actually describes a crossover in temperature. Let us fix $\lambda = 1$ and $T > T_c$. Then y becomes large and positive as $\xi(t_w, T)$ grows. We see that U_4 approach a high-temperature limit (a λ -dependent renormalized coupling constant [50]). At T_c we have the critical limit because $y = 0$ no matter how large $\xi(t_w)$ is. In the spin-glass phase, y becomes large and negative. For large ξ we reach a low-temperature limit, that has been much debated in the past [51,52].

In order to compute the critical exponents, we decided to follow the fixed-height method [53,54]. For a fixed height h , and fixed λ and $\xi(t_w, T)$, we seek the temperature $T_{h,\lambda,\xi}$ such

²Also, we employ *Pthreads* to simulate a single system in multicore processors. Our best timings for $L = 256$ at T_c are: (a) An 8-core Intel(R) Xeon(R) CPU E5-2690: an 8-threads simulation of a single system at 50 ps/spin flip. (b) A single 16-core AMD Opteron (TM) 6272 processor: a 16-threads simulation of a single system at 62 ps/spin flip. For comparison, a single Janus FPGA runs two $L = 80$ systems at 32 ps/spin flip each [20,23].

³Having four replicas at our disposal (eight replicas for $T = 1.1$, 1.25) we average over the 6 (28) possible pairings of replica indices.

⁴Other laws [40] are numerically indistinguishable from a power.

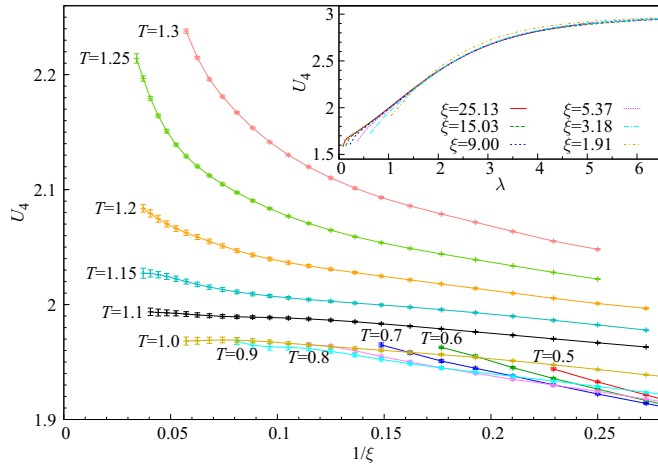


FIG. 2. (Color online) Binder's ratio as a function of $[\xi(t_w, T)]^{-1}$, computed for a fixed dimensionless box size $\lambda = 1$ and several temperatures [recall that $\lambda = l/\xi(t_w)$]. Inset: Critical Binder's ratio as a function of the dimensionless box size for several $\xi(t_w)$ ($T = 1.1 \approx T_c$). As expected by plugging $y = 0$ in Eq. (3), the curve is scale invariant when the small ξ corrections fade away.

that $U_4 = h$. Equation (3) tells us that

$$T_{h,\lambda,\xi} = T_c + A_{h,\lambda}\xi^{-1/\nu} + B_{h,\lambda}\xi^{-(\omega+1/\nu)} \dots, \quad (4)$$

where $A_{h,\lambda}$ and $B_{h,\lambda}$ are scaling amplitudes and the dots stand for higher-order corrections to scaling. We compute T_c , ν , and ω by performing joint fits to data for several λ and h , see Fig. 3 (unfortunately, the fit lacks any predictive power for exponent ω , hence we shall borrow $\omega = 1.12(10)$ from [31]). In order to perform these fits, we considered a fixed grid of coherence lengths $\xi_n = 2^{n/8}$.

A major problem when fitting to Eq. (4) is that of the singular covariance matrix (we have many data points, but only 50 independent samples). We solve it following [20,21]: we fit taking into account only the diagonal part of the covariance matrix. We perform a fit for each jackknife block, and compute the final errors from the fluctuations of these fits. We compute as well the diagonal goodness-of-fit indicator χ_{diagonal}^2 (the sum of the squared deviations of data from fit, in

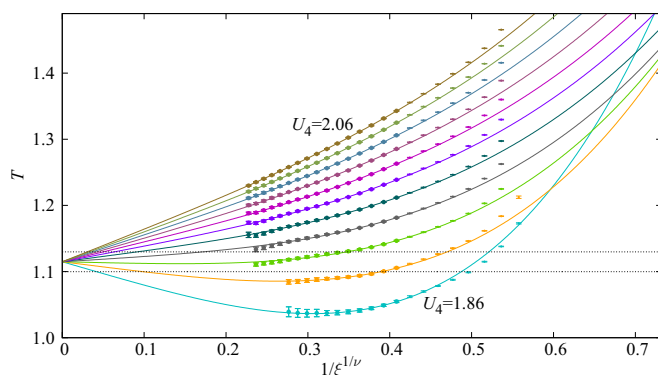


FIG. 3. (Color online) Joint fit to Eq. (4) for $\lambda = 0.75$. The U_4 spacing is 0.02. For all fits, the values of T_c , ν , and ω are held common. Big data points were included in the fit. The horizontal dotted lines correspond to $T_c \pm \Delta T_c$ from Eq. (5).

units of their statistical error). This fitting procedure was tested in Ref. [21] and found to be reasonably stable for χ_{diagonal}^2 as small as half the number of degrees of freedom.

We included in our fit results for $\lambda = 0.75, 1, 1.25$, and 1.5. A crucial issue is selecting ξ_{min} , the minimal ξ considered in the fit. A tradeoff should be found. The larger is ξ_{min} , the smaller are the systematic errors, but the larger becomes the statistical uncertainty. We find a stable fit for $\xi_{\text{min}} \geq 2^{9/4} \approx 4.75$ ($\chi_{\text{diagonal}}^2/\text{d.o.f.} = 583/665$ if $\xi_{\text{min}} = 2^{9/4}$). However, as we enlarge ξ_{min} we find that $\chi_{\text{diagonal}}^2/\text{d.o.f.}$ decreases monotonically while the statistical error increases. We decided to stop at the ξ_{min} such that $\chi_{\text{diagonal}}^2/\text{d.o.f.} \approx 0.5$ because errors start increasing wildly at that point. This corresponds to $\xi_{\text{min}} = 2^{23/8} \approx 7.33$ ($\chi_{\text{diagonal}}^2/\text{d.o.f.} = 229/482$). The final result for our fit to Eq. (4) is

$$T_c = 1.115(15), \quad \nu = 2.2(3). \quad (5)$$

For comparison, recall the equilibrium results $T_c = 1.1019(29)$, $\nu = 2.56(4)$, and $\omega = 1.12(10)$ [31]. Varying ω within the bounds of [31] produces negligible changes in the results in Eq. (5). It is also interesting to see what happens fixing ν and ω in the fit to the central values of [31] ($\xi_{\text{min}} \geq 2^{23/8}$, $\chi_{\text{diagonal}}^2/\text{d.o.f.} = 241/483$):

$$T_c = 1.102(8), \quad (6)$$

in excellent agreement with the equilibrium result.

The anomalous dimension η can be computed by working directly at $T = 1.1 \approx T_c$. We select two times $t_w^{(1)}$ and $t_w^{(2)}$ such that $\xi(t_w^{(1)}, T_c) = \xi$ and $\xi(t_w^{(2)}, T_c) = 2\xi$. Then the ratio of integrals is

$$I_2(t_w^{(2)}, T_c) / I_2(t_w^{(1)}, T_c) = 2^{2-\eta} + C_I / \xi^\omega + \dots \quad (7)$$

The problem with Eq. (7) is that the amplitude for scaling corrections C_I seems vanishing (within errors), so one could be afraid that we overestimate the error. Anyhow, for $\xi_{\text{min}} = 2^{7/4} \approx 3.36$ we obtain $\eta = -0.380(7)$ and $\chi_{\text{diagonal}}^2/\text{d.o.f.} = 10.4/14$, to be compared with $\eta = -0.3900(36)$ [31] (for larger ξ_{min} fits are stable but $\chi_{\text{diagonal}}^2/\text{d.o.f.}$ drops well below 0.5). Changing ω within the bounds of [31] produces a negligible change. We estimate that the error induced in η by the uncertainty in T_c [31] is comparable with the statistical error obtained at $T = 1.1$.

Incidentally, one may use the ratio of integrals $I_2(t_w^{(2)}, T) / I_2(t_w^{(1)}, T)$ as a (very noisy) substitute of the Binder's cumulant in Eqs. (3) and (4) (see Appendix C). In fact, one may view the temperature crossover in Eq. (3) as a crossover for the $C_4(r, t_w)$ correlation function (2). Indeed, for all the T and t_w in this work, the functional form [48]

$$C_4(r, t_w) \sim e^{-[r/\xi(t_w)]^b} / r^\theta \quad (8)$$

satisfactorily fits our data. For small y [i.e., at T_c or for small $\xi(t_w)$] data follows Eq. (8) with critical parameters. However, as the coherence length grows, these parameters are not adequate neither for the paramagnetic phase (at or near equilibrium, see Fig. 4), nor for the spin-glass phase [20,21].

In this work we have employed statics-dynamics equivalence [26] to obtain some new physical results. In particular, we have shown how one can study the spin-glass transition in the dynamic regime relevant to most experiments: nonequilibrium

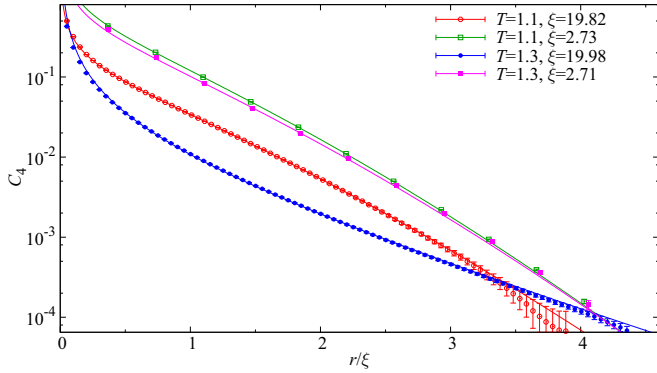


FIG. 4. (Color online) Temperature-dependent dynamic crossover in the spatial correlation function $C_4(r, t_w)$ (2). We show C_4 vs the dimensionless $r/\xi(t_w)$, both at T_c and deep in the paramagnetic phase ($T = 1.3$). For small coherence length $\xi(t_w) \approx 2.7$, data for both temperatures can be fit to Eq. (8) with critical parameters $b \approx 1.46$ (this work) and $\theta \approx D - 2 + \eta = 0.610(4)$ [31], see the continuous lines in the plot. The same parameters work for data at T_c and $\xi(t_w) \approx 20$. However, for such a large coherence length, data at $T = 1.3$ are better fitted with the three-dimensional free-field (Gaussian) parameters ($b = 1, \theta = 1$).

data on systems much larger than the coherence length. Once we trade waiting time by coherence length, standard finite-size scaling methods [46] are very successful at describing the temperature-dependent dynamic crossover (a real phase transition with temperature takes place only for infinite coherence length). It is then possible that the finite-size crossover found in equilibrium [55] is the driving force behind the apparent universality violations found experimentally [12,56–59]. However, an alternative explanation, logically possible but rather dramatic, is that universality does not hold in spin glasses [60,61].

Regarded as a numerical method to compute critical exponents, we note that our thermodynamic limit approach is less accurate than finite-size methods [31,53,62], which is hardly a surprise.

We conclude by mentioning the two major difficulties (in our opinion) for an analogous experimental study. On the one hand, one needs to reach spatial resolution to study the correlation function $C_4(r, t_w)$. Progress in this direction are still incipient. Spatial resolution has been reached only for a structural glass [63]. For spin glasses, recent experimental efforts focus on confining geometries [29,64] (which can be seen as an indirect way to study the correlation function). On the other hand, the direct quench is a rather crude approximation: the experimental sample never reaches the working temperature instantaneously [65,66]. The protocol of Ref. [41] is, probably, more suitable to model the experimental setup. However, as Fig. 1 shows, mixing temperatures in the dynamic evolution is a delicate procedure that requires further investigation.

We thank Enzo Marinari, Giorgio Parisi, and Andrea Maiorano for helping us with our first *Pthreads* programs. We also thank Andrea Pelissetto, Giorgio Parisi, and Matteo Lulli for discussing with us, prior to publication, their

very interesting and accurate *finite-time, finite-size* scaling approach [62]. We thank as well Juan Jesús Ruiz-Lorenzo, Peter Young, and David Yllanes for discussions. The total simulation time devoted to this project was the equivalent of 36 days of the full (3072 AMD cores) *Memento* cluster (see <http://bifi.es>). We were partly supported by MINECO (Spain) through research Contract No. FIS2012-35719-C02.

APPENDIX A: SYNCHRONOUS MULTISPIN CODING

Modern CPUs, both Intel and AMD, support 256-bit words in their streaming extensions. This means that one can perform basic Boolean operations (AND, XOR, etc.) in parallel for all 256 bits. Now, it is well known that the Metropolis update of a single spin can be cast into a sequence of Boolean operations, see, e.g., [67]. One can use this idea to simulate several, up to 256, *independent* systems. This approach, named asynchronous multispin coding, has been used many times, see Refs. [22,31,35,68–70] for instance. References [36,37] offer a creative alternative: In their parallel tempering simulation each bit represents an independent system copy (all of them evolve under the same couplings, but at different temperatures [71,72]). Instead, our aim is to exploit the streaming extensions to speed up the simulation of a *single* system (which is named synchronous multispin coding).

The main problem with synchronous multispin coding is that we need 256 independent random numbers, if the 256 spins coded in a word belong to the same physical system. This breaking of parallelism is usually regarded as a major inconvenience (see, however, Ref. [41]).

For the sake of clarity, we shall first explain our geometrical setup and then describe how one can use the Gillespie method [38,39] to reduce drastically the number of needed random numbers.

1. Our multispin coding geometry

Physical spins sit on the nodes of a $L = 256$ lattice with periodic boundary conditions. Euclidean coordinates then run as $0 \leq x, y, z \leq 255$. Each physical spin is a binary variable to be coded in a single bit, $s_{(x,y,z)} = \pm 1$.

We pack 256 physical spins into one *superspin*. Our superspins sit in the nodes of a different lattice. It will be also a cubic lattice with periodic boundary conditions (the overall geometry is that of a parallelepiped, rather than a cube). The major requirement is that nearest-neighbor spins in the physical lattice should be as well nearest neighbors in the superspin lattice. Our solution is as follows.

Superspins are placed at the nodes of a cubic lattice with dimensions $L_x = L_y = L/8$ and $L_z = L/4$. The relation between physical coordinates (x, y, z) and the coordinates in the superspin lattice (i_x, i_y, i_z) is

$$\begin{aligned} x &= b_x L_x + i_x, & 0 \leq i_x < L_x, & & 0 \leq b_x < 8, \\ y &= b_y L_y + i_y, & 0 \leq i_y < L_y, & & 0 \leq b_y < 8, \\ z &= b_z L_z + i_z, & 0 \leq i_z < L_z, & & 0 \leq b_z < 4. \end{aligned} \quad (\text{A1})$$

In this way, exactly 256 sites in the physical lattice are given the same superspin coordinates (i_x, i_y, i_z) . We differentiate

between them by means of the bit index:

$$i_b = 64b_z + 8b_y + b_x, \quad 0 \leq i_b \leq 255. \quad (\text{A2})$$

An added bonus of Eq. (A1) is that the parity of the original site, namely the parity of $x + y + z$, coincides with the parity of the corresponding superspin site $i_x + i_y + i_z$. In fact, the single cubic lattice is bipartite. It can be regarded as a two interleaved face-centered cubic lattice. A given site is said to belong to the *even* or the *odd* sublattice according to the parity of $x + y + z$. For models with only nearest-neighbors interactions, sites belonging to (say) the even sublattice interact only with the odd sites.

An important consequence of the even-odd decomposition is that it eases parallelism. Indeed, we define the full lattice Metropolis sweep as the update of all the $L^3/2$ even sites, followed by the update of all the $L^3/2$ odd sites. The bipartite nature of the lattice makes it irrelevant the updating order of sites of a given parity. Hence, several updating threads may legitimately concur on the same lattice, provided that all of them simultaneously access only sites of the same parity.

2. Saving random numbers

For our synchronous multispin coding we do need to generate 256 random numbers in order to update a single superspin. Yet, it has been realized several times that most of the effort in generating (pseudo) random numbers is wasted when simulating discrete models at low temperatures [38,39]. In fact, at a given time the simulation may try to overcome an energy barrier ΔE . However, we should overcome it only with probability $e^{-\Delta E/T}$. In other words, we waste $\sim e^{\Delta E/T}$ random numbers (that deny us the permit to overcome the barrier) until we generate one random number that really allows us to walk uphill in energy. Let us plug some numbers for our model, where the possible barrier heights are $\Delta E = 4, 8, \text{ or } 12$. So, at T_c , in the best of cases we use only one random number out of $e^{4/1.1} \approx 38$.

The way out is simple [38,39]: One simulates the random number generator. Indeed, we may regard the random-number generator as a collection of flags. Most of the flags are red (denying us the right to increase the energy), but there is a diluted set of green flags (at sites where the generator does allow us to increase the energy). The trick is setting all flags to red by default, and then caring only of placing green flags with the correct probability.

Before explaining how we simulate our random number generator, let us describe it. By default, let us assume that all flags are red, for all sites and all barriers $\Delta E = 4, 8, \text{ and } 12$. Now, for each site in the physical lattice, we draw one 64-bits uniformly distributed random number: $0 \leq R_4 < 1$. If $R_4 < e^{-4/T}$ then we put a green flag for $\Delta E = 4$ and draw a second uniform random number $0 \leq R_8 < 1$. Now, if $R_8 < e^{-4/T}$ we put a green flag for $\Delta E = 8$,⁵ and draw a *third* uniform random number $0 \leq R_{12} < 1$. Finally, if $R_{12} < e^{-4/T}$ we also put a green flag for $\Delta E = 12$. Of course ours is just an instance among many valid generators. This particular random number generator was chosen because it is fairly easy to simulate.

Let us describe how we simulate the generation of R_4 (the procedure for R_8 and R_{12} are trivial generalizations). We generate an integer $n_4 \geq 0$, with the following meaning: One performs n_4 unfruitful calls to the generator, but on call $1 + n_4$ we should put a green flag. The cumulative probability for n_4 is

$$F(n_4 \leq k) \equiv \text{Prob}(n_4 \leq k) = 1 - (1 - e^{-4/T})^{k+1}. \quad (\text{A3})$$

Hence, we just need to draw an uniform random number $0 \leq R < 1$ and select $n_4 = k$, where k is the non-negative integer that verifies

$$F(k-1) \leq R < F(k) \quad [F(-1) \equiv -1]. \quad (\text{A4})$$

Combining these ideas with the use of look-up tables, we have found that the overall cost of generating random numbers can be made quite bearable.

APPENDIX B: INTERPOLATIONS

The major theme of this work is a change of variable: rather than the the waiting time t_w , we wish to employ the coherence length $\xi(t_w)$. Besides, the quantities computed in the left-hand side of Eq. (3) of the main text were obtained for a discrete set of values of temperatures T , waiting times, and box sizes (l). However, our analysis of the right-hand side of the same equation assumes that the scaling variables $y, \lambda = l/\xi(t_w)$, and $\xi(t_w)$ are continuous. In order to solve this problem we perform several interpolations.

Let us describe our interpolations. In all cases we perform a jackknife error analysis. Let us stress that we are talking here about *interpolations*, rather than extrapolations.⁶

The easiest task is the l interpolation. Data are very smooth (due to their extreme statistical correlation) and a simple cubic spline does an excellent job.

Let us now address $\xi(t_w)$. We take data for times of the form $t_w = [2^{n/4}]$, where n is an integer and $[\dots]$ is the integer part. We find that, even for neighboring times in our logarithmic time mesh, the statistical fluctuations in the coherence length are significant (see Fig. 1). However, we need a monotonously increasing function $\xi(t_w)$ if we are to invert it [that is, to obtain $t_w(\xi)$]. Also it is desirable to have a smooth $\xi(t_w)$ to eliminate the short time-scale fluctuations. Our best solution has been to fit our data to a high-order polynomial in $\log t_w$ (in the fits, see main text, we considered only the diagonal part of the covariance matrix). We checked that $\chi_{\text{diagonal}}^2/\text{d.o.f}$ was smaller than one. However, in order to avoid an excessive data smoothing, we enlarged the degree of the polynomial well beyond that. Basically we stopped before the polynomial became nonmonotonically increasing in the working time range. Notice that our error computation (namely a different fit for each jackknife block) identifies spurious oscillations due to a too large-order fitting polynomial.

Having in our hands an inverse function $t_w(\xi)$ we proceed to compute (using the same fitting approach in $\log t_w$) $U_4(\lambda, \xi, T)$. When needed, see, e.g., Appendix C, we interpolated in the same way the integrals $I_2(t_w)$.

⁵Probability[$R_4 < e^{-4/T}$ and $R_8 < e^{-4/T}$] = $e^{-8/T}$.

⁶Exceptionally we allowed extrapolations no larger than one grid spacing in t_w , or one fourth of the maximum grid spacing in temperature.

Finally, we need to interpolate in T the U_4 values computed at fixed λ and $\xi(t_w)$ for our simulation temperatures. In this case, the variations among neighboring temperatures are typically much larger than error bars. Hence, even a Lagrangian polynomial interpolation works well. However, when the number of data available from the different temperatures is large, we prefer a fit to a low-order polynomial in T . In practice, we restrict ourselves to polynomials of at most fifth degree.

APPENDIX C: DYNAMIC CROSSOVER IN THE CORRELATION FUNCTION

The dynamic crossover (that becomes a true phase transition with the temperature only for infinitely long waiting time) was studied in the main text by focusing on the four-legs correlation function of the overlap field. One could wonder whether one could study the same crossover on the two points correlation function. Indeed, this was the route chosen in Ref. [47] (although the language in Ref. [47] was slightly different).

Let us start by recalling Eqs. (2) and (8):⁷

$$C_4(\mathbf{r}, t_w) \equiv \frac{1}{L^3} \sum_x q_x(t_w) q_{x+\mathbf{r}}(t_w) \sim \frac{e^{-[r/\xi(t_w)]^b}}{r^\theta}. \quad (\text{C1})$$

The asymptotic form in Eq. (C1) is expected to hold only for r much larger than the lattice spacing. Our expectations for the asymptotic regimes.

(1) When we reach equilibrium in the paramagnetic phase, we expect a free-field behavior, namely $\theta = 1$, $b = 1$ in Eq. (C1).

(2) In the critical regime, y of order one {recall from the main text that $y = [T - T_c][\xi(t_w, T)]^{1/\nu}$ or $T = T_c$, we expect $\theta = D - 2 + \eta$, where D is the space dimension and η is the anomalous dimension. We are not aware of any prediction for exponent b . In this work we have found $b = 1.46(1)$.

(3) There is a considerable controversy regarding the spin-glass phase $y \ll -1$. On the one hand, the droplets model [73–76] predicts $\theta = 0$, although the asymptotic limit is reached fairly slowly, with corrections of order $1/\xi^{a \approx 0.2}$. On the other hand, the replica symmetry breaking scenario [15] expects a nontrivial exponent $\theta \approx 0.37$ [26] and corrections of order $1/\xi^\theta$. To our knowledge, neither of the two theories have predictions for exponent b in Eq. (C1). It was empirically found in Ref. [16] that $b \approx 1.5$. In fact, we have found that $b = 1.46(1)$ works just as well in the low temperature phase (see also Ref. [48]).

In order to bypass the unknown exponent b , one may consider the integrals (see [20,21] and main text)

$$I_n(T; t_w) = \int_0^\infty dr r^n C_4(r, t_w, T) \quad (\text{C2})$$

$$\propto \xi^{n+1-\theta} \int_0^\infty du u^{n-\theta} e^{-u^b}. \quad (\text{C3})$$

From them we obtain the integral estimator $\xi_{12} = I_2/I_1 \propto \xi$.

⁷The standard naming *two-legs* or *four-legs* correlation function is somehow confusing in the spin-glass context. In fact, the product of the overlap field at two sites (the two-legs function) involves the product of four spins, hence the name C_4 .

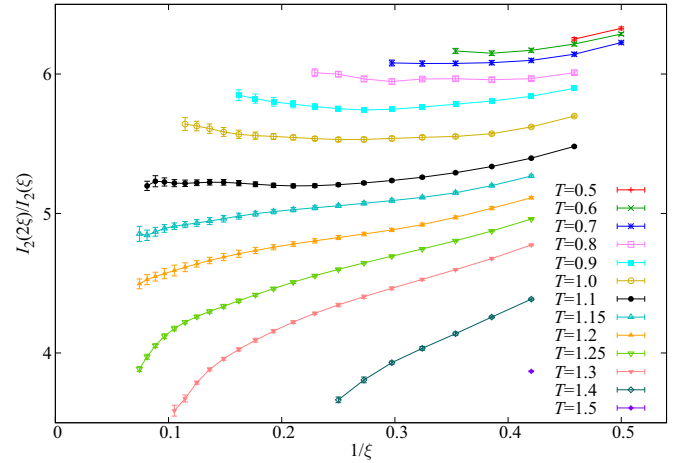


FIG. 5. (Color online) For several temperatures, we plot the susceptibility ratio of Eq. (C5) as a function of the inverse coherence length.

Our analysis will be based on the scaling properties of the integral

$$I_2 \propto \xi_{12}^{3-\theta}. \quad (\text{C4})$$

Note that, in three spatial dimensions, $\chi = 4\pi I_2$, where χ is the (nonequilibrium analog of) the spin-glass susceptibility.⁸ The analysis of Ref. [47] was based on the susceptibility $\chi(T, t_w)$ (however, Ref. [47] did not use the variance reduction methods available for the computation of the integrals I_n [20,21] which are most effective because ξ is much smaller than the system sizes).

As explained in the main text, for any given temperature we may seek two times $t_w^{(1)}$ and $t_w^{(2)}$ such that $\xi_{12}(t_w^{(2)}, T) = 2\xi$, $\xi_{12}(t_w^{(1)}, T) = \xi$.⁹ Hence, for y of order one, we expect

$$I_2(2\xi, T)/I_2(\xi, T) = 2^{2-\eta} f(y) + \dots, \quad (\text{C5})$$

where the scaling function $f(y)$ is such that $f(y = 0) = 1$ and the dots stand for corrections to scaling of order $\xi^{-\omega}$. Note that Eq. (C5) is analogous to Eq. (3) in the main text (where we were considering the Binder's parameter instead).¹⁰

The crossover implicit in Eq. (C5) is shown in Fig. 5, which can be directly compared with Fig. 2. One can consider the $\xi \rightarrow \infty$ limits in the plot.

(1) At the critical point $T = T_c$ one expects $2^{2.3900(36)} = 5.242(13)$ [31].

⁸The relation $\chi = 4\pi I_2$ assumes spatial isotropy in C_4 , which becomes an excellent approximation when ξ grows [21].

⁹One could just as well consider pairs of times such that their coherence lengths are in any prescribed ratio r . In such a case, Eq. (C5) would read as $I_2(r\xi, T)/I_2(\xi, T) = r^{2-\eta} f_r(y) + \dots$.

¹⁰A statistically irrelevant artifact is the presence of wiggles in Fig. 5 if the order of the fitting polynomial in $\log t_w$ is large. The origin of this wiggles has been known for some time [20]. The point is that each polynomial is evaluated twice, one in the numerator and the other in the denominator in Eq. (C5). In fact, the effect can be much alleviated by keeping the order of the polynomial limited to 13. Even with these polynomials, $\chi_{\text{diagonal}}^2/\text{d.o.f.}$ lies well below one.

(2) In the spin-glass phase, the droplets model predict a common limit $2^3 = 8$ for all $T < T_c$, while the replica-symmetry breaking theory expects a limit $2^{\theta_{RSB}} \approx 6.19$.

(3) The paramagnetic phase is more complicated to discuss. In fact, for $T > T_c$, the coherence length grows only up to its equilibrium value for that temperature $\xi_{eq}(T)$. This means that all the (paramagnetic) curves in Fig. 5 have an end point. At this end point the longest time $t_w^{(2)}$ corresponds to

the equilibrium regime (i.e., $\theta_2 = 1$), while the earliest time is still in the nonequilibrium regime. Hence it is not easy to anticipate the numerical value of the paramagnetic long-time limit, obtained when $\xi_{eq}(T)$ tends to infinity.

Data in Fig. 5 can be analyzed in exactly the same way we did for the Binder's parameter [see Eq. (4) and Fig. 3]. However, with the susceptibility ratio Eq. (C5), errors are one order of magnitude larger. This is why we abandoned this approach.

-
- [1] A. Cavagna, *Phys. Rep.* **476**, 51 (2009).
- [2] G. Adam and J. H. Gibbs, *J. Chem. Phys.* **43**, 139 (1965).
- [3] E. R. Weeks, J. C. Crocker, A. C. Levitt, A. Schofield, and D. A. Weitz, *Science* **287**, 627 (2000).
- [4] L. Berthier, G. Biroli, J.-P. Bouchaud, L. Cipelletti, D. El Masri, D. L'Hôte, F. Ladieu, and M. Pierno, *Science* **310**, 1797 (2005).
- [5] R. Gutiérrez, S. Karmakar, Y. G. Pollack, and I. Procaccia, [arXiv:1409.5067](https://arxiv.org/abs/1409.5067).
- [6] K. Gunnarsson, P. Svedlindh, P. Nordblad, L. Lundgren, H. Aruga, and A. Ito, *Phys. Rev. B* **43**, 8199 (1991).
- [7] M. Palassini and S. Caracciolo, *Phys. Rev. Lett.* **82**, 5128 (1999).
- [8] H. G. Ballesteros, A. Cruz, L. A. Fernandez, V. Martin-Mayor, J. Pech, J. J. Ruiz-Lorenzo, A. Tarancon, P. Tellez, C. L. Ullod, and C. Ungil, *Phys. Rev. B* **62**, 14237 (2000).
- [9] E. Vincent, J. Hammann, M. Ocio, J.-P. Bouchaud, and L. F. Cugliandolo, in *Complex Behavior of Glassy Systems*, Lecture Notes in Physics No. 492, edited by M. Rubí and C. Pérez-Vicente (Springer, Berlin, 1997).
- [10] A. J. Bray, *Adv. Phys.* **43**, 357 (1994).
- [11] Y. G. Joh, R. Orbach, G. G. Wood, J. Hammann, and E. Vincent, *Phys. Rev. Lett.* **82**, 438 (1999).
- [12] F. Bert, V. Dupuis, E. Vincent, J. Hammann, and J.-P. Bouchaud, *Phys. Rev. Lett.* **92**, 167203 (2004).
- [13] H. Rieger, *J. Phys. A* **26**, L615 (1993).
- [14] J. Kisker, L. Santen, M. Schreckenberg, and H. Rieger, *Phys. Rev. B* **53**, 6418 (1996).
- [15] E. Marinari, G. Parisi, F. Ricci-Tersenghi, J. J. Ruiz-Lorenzo, and F. Zuliani, *J. Stat. Phys.* **98**, 973 (2000).
- [16] E. Marinari, G. Parisi, F. Ricci-Tersenghi, and J. J. Ruiz-Lorenzo, *J. Phys. A* **33**, 2373 (2000).
- [17] L. Berthier and J.-P. Bouchaud, *Phys. Rev. B* **66**, 054404 (2002).
- [18] L. Berthier and A. P. Young, *Phys. Rev. B* **71**, 214429 (2005).
- [19] L. C. Jaubert, C. Chamon, L. F. Cugliandolo, and M. Picco, *J. Stat. Mech.* (2007) P05001.
- [20] F. Belletti, M. Cotallo, A. Cruz, L. A. Fernandez, A. Gordillo-Guerrero, M. Guidetti, A. Maiorano, F. Mantovani, E. Marinari, V. Martin-Mayor, A. M. Sodupe, D. Navarro, G. Parisi, S. Perez-Gaviro, J. J. Ruiz-Lorenzo, S. F. Schifano, D. Sciretti, A. Tarancon, R. Tripiccone, J. L. Velasco, and D. Yllanes (Janus Collaboration), *Phys. Rev. Lett.* **101**, 157201 (2008).
- [21] F. Belletti, A. Cruz, L. A. Fernandez, A. Gordillo-Guerrero, M. Guidetti, A. Maiorano, F. Mantovani, E. Marinari, V. Martin-Mayor, J. Monforte, A. Muñoz Sodupe, D. Navarro, G. Parisi, S. Perez-Gaviro, J. J. Ruiz-Lorenzo, S. F. Schifano, D. Sciretti, A. Tarancon, R. Tripiccone, and D. Yllanes (Janus Collaboration), *J. Stat. Phys.* **135**, 1121 (2009).
- [22] M. Manssen and A. K. Hartmann, [arXiv:1411.5512](https://arxiv.org/abs/1411.5512).
- [23] F. Belletti, M. Cotallo, A. Cruz, L. A. Fernandez, A. Gordillo, A. Maiorano, F. Mantovani, E. Marinari, V. Martin-Mayor, A. Muñoz Sodupe, D. Navarro, S. Perez-Gaviro, J. J. Ruiz-Lorenzo, S. F. Schifano, D. Sciretti, A. Tarancon, R. Tripiccone, and J. L. Velasco (Janus Collaboration), *Comput. Phys. Commun.* **178**, 208 (2008).
- [24] S. Franz, M. Mézard, G. Parisi, and L. Peliti, *Phys. Rev. Lett.* **81**, 1758 (1998).
- [25] A. Barrat and L. Berthier, *Phys. Rev. Lett.* **87**, 087204 (2001).
- [26] R. Alvarez Baños, A. Cruz, L. A. Fernandez, J. M. Gil-Narvion, A. Gordillo-Guerrero, M. Guidetti, A. Maiorano, F. Mantovani, E. Marinari, V. Martin-Mayor, J. Monforte-Garcia, A. Muñoz Sodupe, D. Navarro, G. Parisi, S. Perez-Gaviro, J. J. Ruiz-Lorenzo, S. F. Schifano, B. Seoane, A. Tarancon, R. Tripiccone, and D. Yllanes (Janus Collaboration), *Phys. Rev. Lett.* **105**, 177202 (2010).
- [27] P. E. Jönsson, H. Yoshino, P. Nordblad, H. Aruga Katori, and A. Ito, *Phys. Rev. Lett.* **88**, 257204 (2002).
- [28] S. Nakamae, C. Crauste-Thibierge, D. L'Hôte, E. Vincent, E. Dubois, V. Dupuis, and R. Perzynski, *Appl. Phys. Lett.* **101**, 242409 (2012).
- [29] S. Guchhait and R. Orbach, *Phys. Rev. Lett.* **112**, 126401 (2014).
- [30] M. Hasenbusch, A. Pelissetto, and E. Vicari, *J. Stat. Mech.* (2008) L02001.
- [31] M. Baity-Jesi, R. A. Baños, A. Cruz, L. A. Fernandez, J. M. Gil-Narvion, A. Gordillo-Guerrero, D. Iñiguez, A. Maiorano, F. Mantovani, E. Marinari, V. Martin-Mayor, J. Monforte-Garcia, A. Muñoz Sodupe, D. Navarro, G. Parisi, S. Perez-Gaviro, M. Pivanti, F. Ricci-Tersenghi, J. J. Ruiz-Lorenzo, S. F. Schifano, B. Seoane, A. Tarancon, R. Tripiccone, and D. Yllanes (Janus Collaboration), *Phys. Rev. B* **88**, 224416 (2013).
- [32] Y. Ozeki and N. Ito, *J. Phys. A: Math. Theor.* **40**, R149 (2007).
- [33] P. Hohenberg and B. Halperin, *Rev. Mod. Phys.* **49**, 435 (1977).
- [34] D. P. Landau and K. Binder, *A Guide to Monte Carlo Simulations in Statistical Physics*, 2nd ed. (Cambridge University Press, Cambridge, 2005).
- [35] M. Lulli, M. Bernaschi, and G. Parisi, [arXiv:1411.0127](https://arxiv.org/abs/1411.0127).
- [36] Y. Fang, S. Feng, K.-M. Tam, Z. Yun, J. Moreno, J. Ramanujam, and M. Jarrell, *Comput. Phys. Commun.* **185**, 2467 (2014).
- [37] S. Feng, Y. Fang, K.-M. Tam, Z. Yun, J. Ramanujam, J. Moreno, and M. Jarrell, [arXiv:1403.4560](https://arxiv.org/abs/1403.4560).
- [38] D. T. Gillespie, *J. Phys. Chem.* **81**, 2340 (1977).
- [39] A. B. Bortz, M. H. Kalos, and J. L. Lebowitz, *J. Comput. Phys.* **17**, 10 (1975).
- [40] J.-P. Bouchaud, V. Dupuis, J. Hammann, and E. Vincent, *Phys. Rev. B* **65**, 024439 (2001).
- [41] C.-W. Liu, A. Polkovnikov, A. Sandvik, and A. P. Young, [arXiv:1411.6745](https://arxiv.org/abs/1411.6745).
- [42] M. P. Nightingale and H. W. J. Blöte, *Phys. Rev. B* **62**, 1089 (2000).

- [43] J. A. Mydosh, *Spin Glasses: An Experimental Introduction* (Taylor and Francis, London, 1993).
- [44] T. Nakamura, S.-i. Endoh, and T. Yamamoto, *J. Phys. A* **36**, 10895 (2003).
- [45] F. Romá, *Phys. Rev. B* **82**, 212402 (2010).
- [46] K. Binder, *Z. Phys. B Condens. Matter* **43**, 119 (1981).
- [47] T. Nakamura, *Phys. Rev. B* **82**, 014427 (2010).
- [48] E. Marinari, G. Parisi, J. Ruiz-Lorenzo, and F. Ritort, *Phys. Rev. Lett.* **76**, 843 (1996).
- [49] D. J. Amit and V. Martin-Mayor, *Field Theory, the Renormalization Group and Critical Phenomena*, 3rd ed. (World Scientific, Singapore, 2005).
- [50] G. Parisi, *Statistical Field Theory* (Addison-Wesley, Reading, MA, 1988).
- [51] E. Marinari, G. Parisi, F. Ricci-Tersenghi, and J. J. Ruiz-Lorenzo, *J. Phys. A* **31**, L481 (1998).
- [52] C. M. Newman and D. L. Stein, *Phys. Rev. E* **57**, 1356 (1998).
- [53] M. Hasenbusch, A. Pelissetto, and E. Vicari, *Phys. Rev. B* **78**, 214205 (2008).
- [54] R. A. Baños, A. Cruz, L. A. Fernandez, J. M. Gil-Narvion, A. Gordillo-Guerrero, M. Guidetti, D. Iniguez, A. Maiorano, E. Marinari, V. Martin-Mayor, J. Monforte-Garcia, A. Muñoz Sudupe, D. Navarro, G. Parisi, S. Perez-Gaviro, J. J. Ruiz-Lorenzo, S. F. Schifano, B. Seoane, A. Tarancon, P. Tellez, R. Tripiccione, and D. Yllanes, *Proc. Natl. Acad. Sci. USA* **109**, 6452 (2012).
- [55] M. Baity-Jesi, L. A. Fernandez, V. Martin-Mayor, and J. M. Sanz, *Phys. Rev. B* **89**, 014202 (2014).
- [56] H. Bouchiat, *J. Phys. France* **47**, 71 (1986).
- [57] L. P. Lévy, *Phys. Rev. B* **38**, 4963 (1988).
- [58] D. Petit, L. Fruchter, and I. A. Campbell, *Phys. Rev. Lett.* **88**, 207206 (2002).
- [59] I. A. Campbell and D. C. M. C. Petit, *J. Phys. Soc. Jpn.* **79**, 011006 (2010).
- [60] P. O. Mari and I. A. Campbell, *Phys. Rev. E* **59**, 2653 (1999).
- [61] M. Pleimling and I. A. Campbell, *Phys. Rev. B* **72**, 184429 (2005).
- [62] M. Lulli, G. Parisi, and A. Pelissetto (unpublished).
- [63] H. Oukris and N. E. Israeloff, *Nat. Phys.* **6**, 135 (2010).
- [64] K. Komatsu, D. L'Hôte, S. Nakamae, V. Mosser, M. Konczykowski, E. Dubois, V. Dupuis, and R. Perzynski, *Phys. Rev. Lett.* **106**, 150603 (2011).
- [65] G. F. Rodriguez, G. G. Kenning, and R. Orbach, *Phys. Rev. Lett.* **91**, 037203 (2003).
- [66] G. F. Rodriguez, G. G. Kenning, and R. Orbach, *Phys. Rev. B* **88**, 054302 (2013).
- [67] M. E. J. Newman and G. T. Barkema, *Monte Carlo Methods in Statistical Physics* (Clarendon Press, Oxford, 1999).
- [68] L. Leuzzi, G. Parisi, F. Ricci-Tersenghi, and J. J. Ruiz-Lorenzo, *Phys. Rev. Lett.* **101**, 107203 (2008).
- [69] R. A. Baños, L. A. Fernandez, V. Martin-Mayor, and A. P. Young, *Phys. Rev. B* **86**, 134416 (2012).
- [70] L. A. Fernandez, V. Martin-Mayor, G. Parisi, and B. Seoane, *Phys. Rev. B* **81**, 134403 (2010).
- [71] K. Hukushima and K. Nemoto, *J. Phys. Soc. Jpn.* **65**, 1604 (1996).
- [72] E. Marinari, in *Advances in Computer Simulation*, edited by J. Kerstész and I. Kondor (Springer, Berlin, 1998).
- [73] W. L. McMillan, *J. Phys. C: Solid State Phys.* **17**, 3179 (1984).
- [74] A. J. Bray and M. A. Moore, in *Heidelberg Colloquium on Glassy Dynamics*, Lecture Notes in Physics No. 275, edited by J. L. van Hemmen and I. Morgenstern (Springer, Berlin, 1987).
- [75] D. S. Fisher and D. A. Huse, *Phys. Rev. Lett.* **56**, 1601 (1986).
- [76] D. S. Fisher and D. A. Huse, *Phys. Rev. B* **38**, 386 (1988).